

# Design and Performance of Rate-compatible Non-Binary LDPC Convolutional Codes

Hironori Uchikawa, Kenta Kasai and Kohichi Sakaniwa  
Dept. of Communications and Integrated Systems  
Tokyo Institute of Technology  
152-8550 Tokyo, JAPAN  
Email: {uchikawa, kenta, sakaniwa}@comm.ss.titech.ac.jp

**Abstract**—In this paper, we present a construction method of non-binary low-density parity-check (LDPC) convolutional codes. Our construction method is an extension of Felström and Zigangirov construction [1] for non-binary LDPC convolutional codes. The rate-compatibility of the non-binary convolutional code is also discussed. The proposed rate-compatible code is designed from one single mother (2,4)-regular non-binary LDPC convolutional code of rate 1/2. Higher-rate codes are produced by puncturing the mother code and lower-rate codes are produced by multiplicatively repeating the mother code. Simulation results show that non-binary LDPC convolutional codes of rate 1/2 outperform state-of-the-art binary LDPC convolutional codes with comparable constraint bit length. Also the derived low-rate and high-rate non-binary LDPC convolutional codes exhibit good decoding performance without loss of large gap to the Shannon limits.

## I. INTRODUCTION

Low-density parity-check (LDPC) block codes were first invented by Gallager [2]. Optimized binary LDPC block codes can approach very close to the Shannon limit with long code lengths [3]. Non-binary LDPC block codes were also invented by Gallager [2]. Davey and MacKay [4] found non-binary LDPC codes can outperform binary ones. Non-binary LDPC block codes have captured much attention recently due to their decoding performance for moderate code lengths and their rate-compatibility [5].

The convolutional counterparts of LDPC block codes, namely LDPC convolutional codes were proposed in [1]. LDPC convolutional codes are suitable for packet based communication systems with variable length frames, since LDPC convolutional codes can be employed to construct a family of codes of varying frame length via termination at both encoder and decoder. Felström and Zigangirov constructed the time-varying periodic LDPC convolutional codes from LDPC block codes [1]. Surprisingly, the LDPC convolutional codes outperform the constituent underlying LDPC block codes. Recently, Kudekar *et al.* investigated such decoding performance improvement by using GEXIT and showed that the terminated LDPC convolutional coding increases the belief propagation (BP) threshold, a maximum channel parameter at which decoding error probability goes to an arbitrarily small as the code length tends to infinity, up to the maximum a-priori (MAP) threshold of the underlying block code [6]. In order to achieve capacity approaching performance, LDPC

convolutional codes need to have a long constraint length, however the long constraint length leads to long decoding latency [7]. The long latency is not preferred for real time communication systems. Moreover it is desired to design rate-compatible convolutional codes that cover from low rate to high rate, to establish reliable communication systems over channels with wide range of noise strength.

In this paper, we study a non-binary LDPC convolutional code and its rate-compatibility. We modify the construction method [1], in order to construct a non-binary (2,4)-regular LDPC convolutional code. Using the (2,4)-regular LDPC convolutional code as a mother code, a rate-compatible non-binary LDPC convolutional code can be derived. High-rate non-binary LDPC convolutional codes are produced by puncturing the mother LDPC convolutional code. Lower-rate codes are produced by multiplicatively repeating the mother code [5]. Simulation results show the non-binary LDPC convolutional code of rate 1/2 outperforms binary LDPC convolutional codes with smaller decoding latency, and also have good performance for rates from 1/4 to 7/8 without large loss from the Shannon limits.

The paper is organized as follows. In Section II, we introduce terminated LDPC convolutional codes over  $\text{GF}(2^p)$ . Then we give a construction method and simulation results for a mother 1/2 code in Section III. Section IV explains how to produce low-rate codes and high-rate codes from the mother code. Finally, we give conclusions in Section V.

## II. TERMINATED LDPC CONVOLUTIONAL CODES OVER $\text{GF}(2^p)$

In this section, we present a brief overview of terminated  $(m_s, J, K)$  regular LDPC convolutional codes over  $\text{GF}(2^p)$ .

### A. Code Definition

For convenience, we follow the notations in [8] to describe time-varying syndrome former (transposed parity-check) matrix of LDPC convolutional codes. An  $(m_s, J, K)$  regular LDPC convolutional code over  $\text{GF}(2^p)$  is the set of sequences  $\mathbf{v} \in \text{GF}(2^p)^{c(N+Z)}$  satisfying the equation  $\mathbf{v}\mathbf{H}^T = \mathbf{0}$ , where  $Z$  is a time unit for termination. The length of the codeword  $\mathbf{v}$  is given as  $c(N+Z)$ . A syndrome former matrix  $\mathbf{H}^T$  is defined as (2). The submatrix  $\mathbf{H}_i^T(t)$ ,  $i = 0, 1, \dots, m_s$ , is a

$c \times (c - b)$  non-binary matrix over  $\text{GF}(2^p)$  which forms

$$\mathbf{H}_i^T(t) = \begin{bmatrix} h_i^{(1,1)}(t) & \cdots & h_i^{(1,c-b)}(t) \\ \vdots & & \vdots \\ h_i^{(c,1)}(t) & \cdots & h_i^{(c,c-b)}(t) \end{bmatrix}, \quad (1)$$

where  $h_i^{(\gamma,\eta)}(t) \in \text{GF}(2^p)$ , for  $\gamma = 1, \dots, c$ ,  $\eta = 1, \dots, c - b$ ,  $p \geq 2$ .  $\mathbf{H}_0^T(t)$  needs to be full rank for systematic encoding and  $\mathbf{H}_{m_s}^T(t)$  should be a nonzero matrix to maintain a constraint length  $\nu_s = (m_s + 1)c$ .  $m_s$  is the maximum width of the nonzero entries in the matrix  $\mathbf{H}^T$ , and is referred to as syndrome former memory, associated constraint bit length is defined as  $\nu_b = (m_s + 1)cp$ .

In a practical manner, a syndrome former matrix has a periodical structure. Therefore  $\mathbf{H}_i^T(t) = \mathbf{H}_i^T(t+T)$  is satisfied for all  $t$ , where  $T$  is called the period of the matrix. For large  $N$ , the rate  $R$  of this code is given as

$$R = \frac{b}{c(1 + Z/N)} = \frac{b}{c} \quad (N \rightarrow \infty)$$

$\mathbf{H}^T$  has  $J$  nonzero entries in each row and  $K$  nonzero entries in each column, except at the first  $m_s(c - b)$  columns and the last  $Z$  columns.

### B. Encoding

Encoding of the non-binary LDPC convolutional codes is accomplished in a systematic manner. Let  $\mathbf{u}$  be the information sequence, where

$$\begin{aligned} \mathbf{u} &:= (\mathbf{u}_0, \mathbf{u}_1, \dots, \mathbf{u}_t, \dots, \mathbf{u}_{N+Z-1}) \in \text{GF}(2^p)^{b(N+Z)}, \\ \mathbf{u}_t &:= (u_t^{(1)}, \dots, u_t^{(b)}) \in \text{GF}(2^p)^b. \end{aligned}$$

This information sequence is encoded into the coded sequence  $\mathbf{v}$  by a convolutional encoder, where

$$\begin{aligned} \mathbf{v} &:= (\mathbf{v}_0, \mathbf{v}_1, \dots, \mathbf{v}_t, \dots, \mathbf{v}_{N+Z-1}) \in \text{GF}(2^p)^{c(N+Z)}, \\ \mathbf{v}_t &:= (v_t^{(1)}, \dots, v_t^{(c)}) \in \text{GF}(2^p)^c. \end{aligned}$$

The coded sequence satisfies  $\mathbf{v}\mathbf{H}^T = \mathbf{0}$  which can be rewritten as

$$\sum_{i=0}^t \mathbf{v}_{t-i} \mathbf{H}_i^T(t) = 0, \quad \text{for } 0 \leq t < m_s, \quad (3)$$

$$\sum_{i=0}^{m_s} \mathbf{v}_{t-i} \mathbf{H}_i^T(t) = 0, \quad \text{for } m_s \leq t \leq N + Z - 1. \quad (4)$$

To obtain a systematic non-binary LDPC convolutional code, the last  $(c - b)$  rows of  $\mathbf{H}_0^T(t)$  are chosen so as to be a  $(c - b) \times (c - b)$  diagonal matrix [9]. The code sequence  $\mathbf{v}$  can be calculated using Eqs. (3), (4) by the expressions

$$\begin{aligned} v_t^{(j)} &= u_t^{(j)}, \quad \text{for } j = 1, \dots, b, \\ v_t^{(j)} &= \frac{\sum_{k=1}^b v_t^{(k)} h_0^{(k,j-b)}(t) + \sum_{i=1}^{m_s} \sum_{k=1}^c v_{t-i}^{(k)} h_i^{(k,j-b)}(t)}{h_0^{(j,j-b)}(t)}, \\ &\quad \text{for } j = b + 1, \dots, c. \end{aligned}$$

This can be easily implemented with shift registers. For example, the encoder of a non-binary LDPC convolutional code with  $R = b/c = 1/2$  is depicted in Fig. 1. The number of required memory bits is equal to  $((m_s c) + b)p$  and the average complexity to encode one parity symbol is proportional to  $K - 1$ . The encoding complexity is independent of the codeword length and the syndrome former memory  $m_s$ . A straightforward encoder for a length  $N$  non-binary LDPC block code has a complexity per parity bit of  $O(N)$ , since the encoder multiplies the information sequence by the generator matrix. Therefore the non-binary LDPC convolutional codes have a significant advantage compared to non-binary LDPC block codes in terms of encoding complexity.

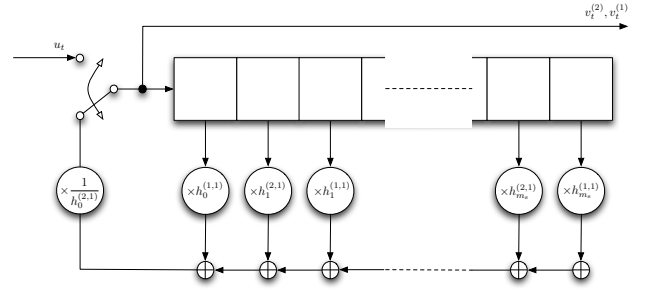


Fig. 1. A shift register based encoder for non-binary LDPC convolutional codes with  $R = 1/2$

### C. Decoding

Decoding of the non-binary LDPC convolutional codes can be performed in several ways. A message passing algorithm similar to that for non-binary LDPC block codes is applicable, since the non-binary LDPC convolutional codes discussed in this paper are terminated. However we have a special algorithm called sliding windowed decoding for the non-binary LDPC convolutional codes [7]. Due to the convolutional structure, the distance between two variable nodes that are connected to the same check node is limited by the memory of the code. This property can be used in order to perform continuous decoding of the received sequence through a window that slides along the sequence, analogous to the Viterbi decoder with finite path memory. Since the sliding windowed decoder does not need message memory for the entire code sequence, it has the advantage compared to the decoder of the LDPC block codes in terms of decoder complexity,

Moreover the decoding of two variable nodes that are at least  $(m_s + 1)$  time units apart can be performed independently, since the corresponding symbols cannot be involved in the same parity-check equations. This indicates the possibility of parallelizing the iterations of the message passing decoder, through several processors working in different regions of the Tanner graph. A pipeline decoder based on this idea was proposed in [1]. Figure 2 shows a sliding windowed decoder for  $(5, 2, 4)$  non-binary LDPC convolutional code for an example. The decoding time for each symbol in the decoding window is proportional to  $(m_s + 1)cI$ , where  $I$  represents



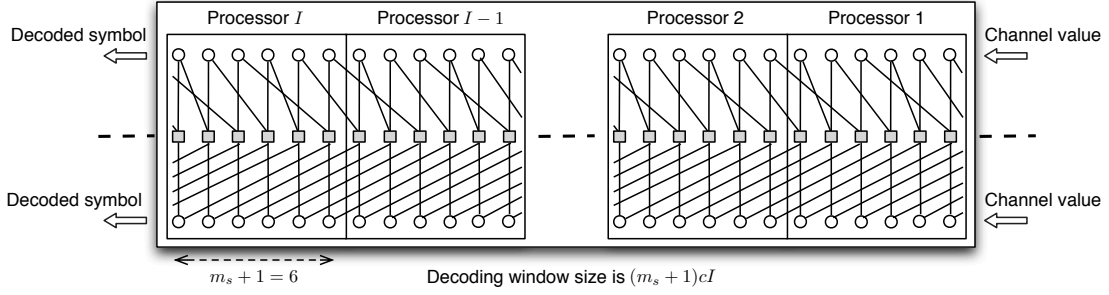


Fig. 2. A sliding windowed decoder for (5, 2, 4) non-binary LDPC convolutional code with  $R = 1/2$

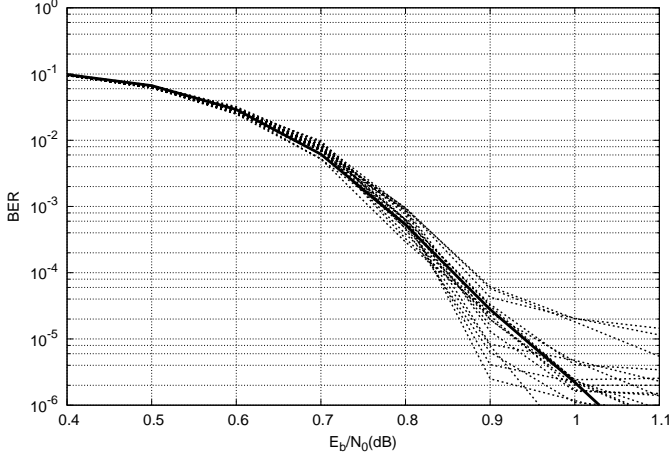


Fig. 3. Bit error rate (BER) of 20 instances of (52, 2, 4) LDPC convolutional code over  $GF(2^8)$ . The code of the solid line is used in the following section. We observe that the average of the error floor performance is between  $10^{-5}$  and  $10^{-6}$ .

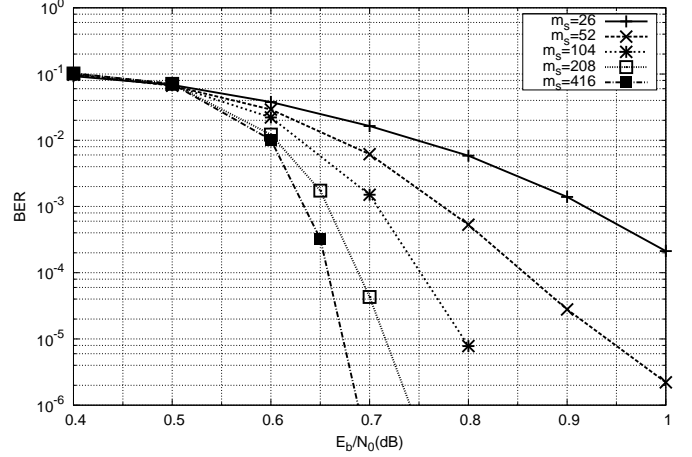


Fig. 4. The BER performances of  $m_s = 26, 52, 104, 208,$  and  $416, J = 2, K = 4$  non-binary LDPC convolutional code over  $GF(2^8)$ . All of these codes are rate  $1/2$ . Error correction performance improves with increasing  $m_s$ .

the BER of  $10^{-4}$  because of the dispersion of the error floor performance. Since the BER curve of the code is the average of 20 instances, we employ the code of the solid line in the following section. Also we believe that generating 20 instances is enough to obtain the average error performance code by using our construction method.

In general, the binary LDPC convolutional codes with large  $m_s$ , i.e., large  $\nu_b$  have good error correction performance. The binary LDPC convolutional codes with  $\nu_b > 2000$  were discussed in [8] [9]. From Fig. 4, we can claim the same statement for the non-binary LDPC convolutional codes. In the point of view of the error correcting performance, large  $\nu_b$  is preferred, however we expect that such codes have large decoding latency. In order to show the superior performance of our proposed codes, we will employ the non-binary LDPC convolutional codes with small  $\nu_b = 848$ , i.e.,  $m_s = 52$  in this paper. Simulation results show that the non-binary LDPC convolutional codes have good error correction performance, nevertheless such small  $\nu_b$ .

### B. Simulation Results

In this section, we compare the non-binary LDPC convolutional codes with binary LDPC convolutional codes and non-

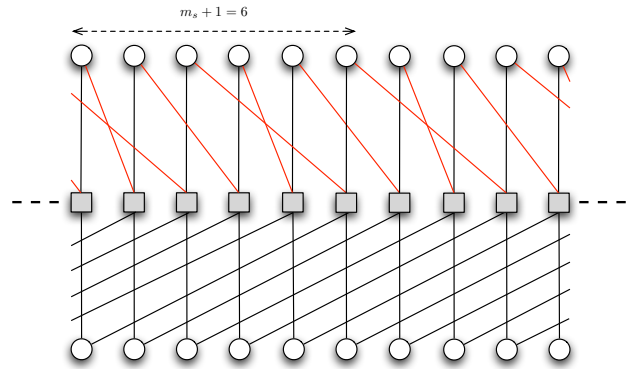


Fig. 6. Tanner graph of (5,2,4)-regular LDPC convolutional code

binary LDPC block codes.

The transmissions over the AWGN channel with BPSK are assumed. The sum-product algorithm using the fast Fourier transform (FFT) is employed for decoding. The number of iterations is set to 50.

In Fig. 7, we compare the BER of a (52, 2, 4) LDPC convolutional code over  $GF(2^8)$  with binary LDPC convolutional

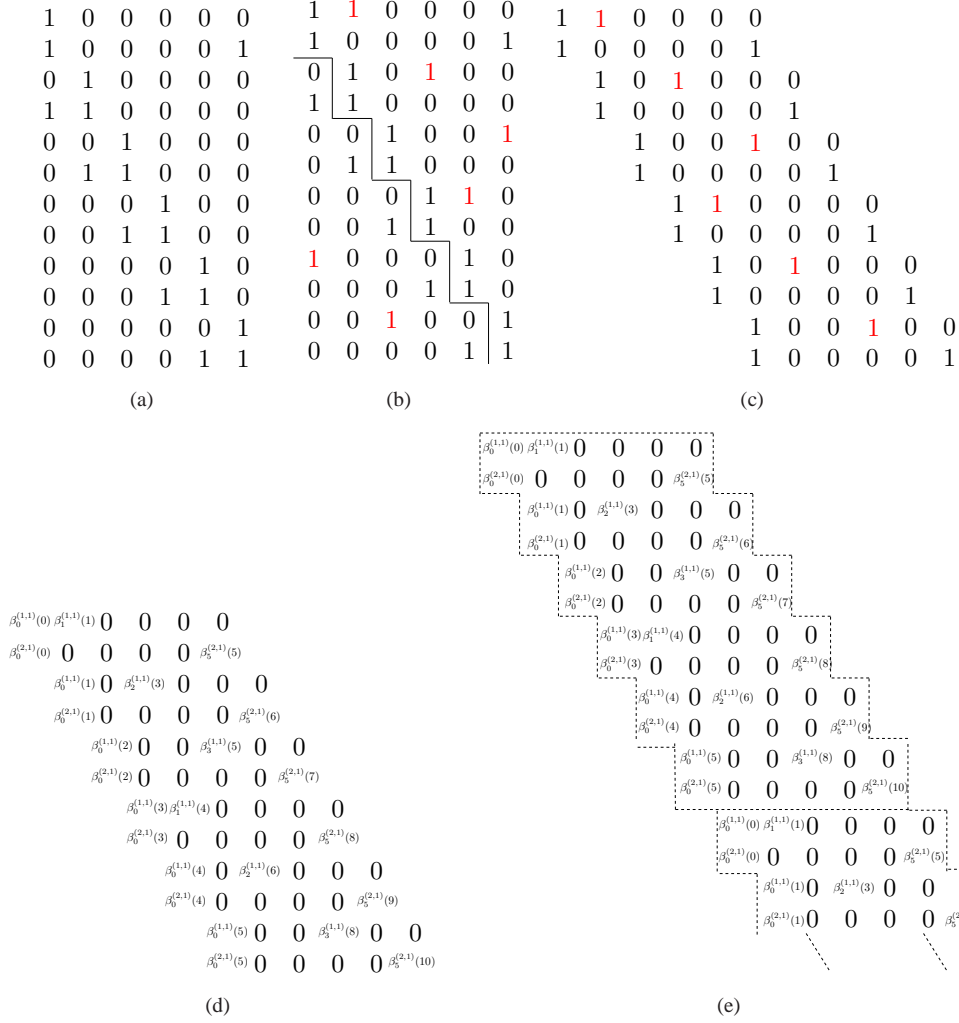


Fig. 5. Construction procedure of a (5,2,4)-regular non-binary LDPC convolutional code.

codes. In the simulation, the termination time unit  $Z$  is set to  $m_s$ . Therefore the termination bit length of the (52, 2, 4) LDPC convolutional code over  $\text{GF}(2^8)$  is 832. The encoded information bit length  $bpN$  is set to 40000. The resulting code rate is almost 0.495.

For the binary convolutional codes, one is a (3,6) regular LDPC convolutional code [7] and the other is a terminated accumulate-repeat-jagged-accumulate (TARJA) convolutional code [12]. Both codes are expanded from their protograph with random permutation matrices of sizes  $M = 142$  and 212, making their constraint bit lengths equivalent to the non-binary code. Both binary LDPC convolutional codes with 5 times longer constraint bit length are also shown for comparison. Termination factor  $L$  is set to make their code rates equivalent to the rate of the non-binary code. It is observed that the (52, 2, 4) non-binary LDPC convolutional code provides superior performance (about 0.3 dB at a BER of  $10^{-4}$ ) with smaller decoding latency to the state-of-the-art binary TARJA convolutional code ( $M = 1060, L = 50$ ). Also it can be seen that the non-binary code does not have error floors down to

BER  $10^{-5}$ .

Figure 8 shows the performances of two (2, 4) LDPC block codes over  $\text{GF}(2^8)$ , which have the symbol nodes of degree 2 and the check nodes of the degree 4. The block lengths were chosen so that in one case the decoders have the same processor complexity [8], i.e.,  $N = \nu_s$ , and in the other case the same memory requirements, i.e.,  $N = \nu_s \cdot I$ . For the same processor complexity, the convolutional code outperforms the block code by about 0.9 dB at a BER of  $10^{-4}$ . However the block code outperforms the convolutional code by about 0.15 dB at a BER of  $10^{-4}$  for the same memory requirements. In binary cases, the convolutional code slightly outperforms the block code for the same memory requirements [8]. However this is not the case of non-binary codes in our simulation result. We will discuss this phenomenon in the next section.

### C. Discussion and BP threshold analysis

In order to explain the reason why the bit error rate performance of the non-binary LDPC convolutional codes is worse than the corresponding block codes in the previous section,

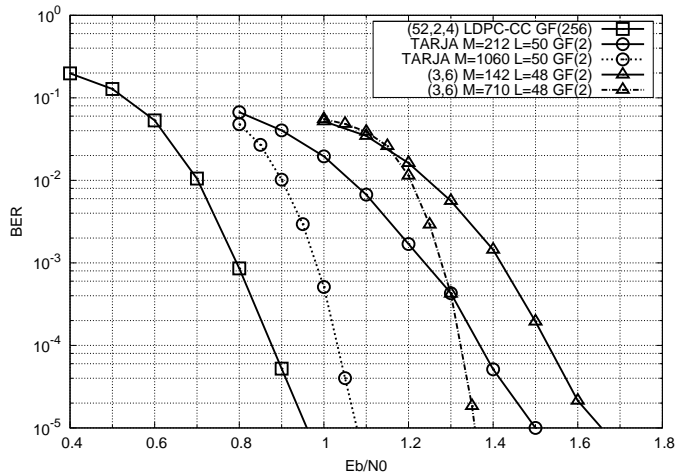


Fig. 7. Simulation results of a (52, 2, 4) LDPC convolutional code over  $GF(2^8)$  (square), a binary TARJA convolutional code [12] (circle), and a binary (3,6) convolutional code (triangle). Both binary codes are constructed with equivalent constraint bit length  $\nu_b = 848$  (solid lines) to the non-binary code and 5 times longer constraint bit length (dashed lines). All of these codes are of rate 1/2.

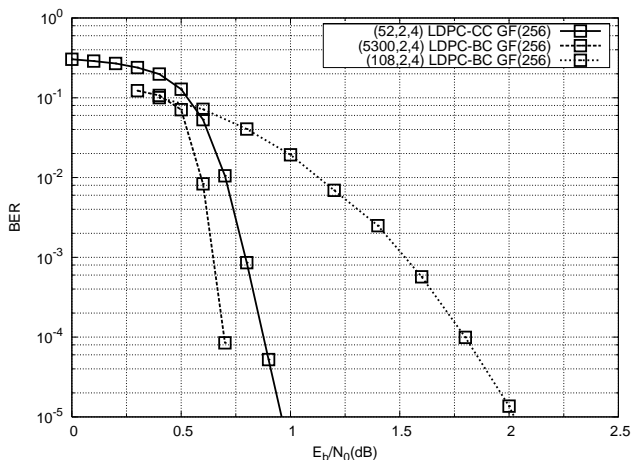


Fig. 8. Simulation results of a (52, 2, 4) LDPC convolutional code (CC) (solid lines) with same memory requirements and processor complexity,  $N = 5300$  and 108 respectively, LDPC block codes (BC) (dashed lines). All of these codes are of rate 1/2 and defined over  $GF(2^8)$ .

we show another simulation result and also numerical calculation of the BP threshold. In Fig. 9, we provide simulation results of non-binary LDPC convolutional codes of different degrees of symbol nodes and block codes with comparable memory requirements. With an abuse of notation, a (52, 2.5, 5) convolutional code and a (5300, 2.5, 5) block code have equivalent number of symbol nodes of degree 2 and 3, so that the average degrees of symbol nodes are 2.5. In other words, the syndrome former matrix of  $J = 2.5$  convolutional codes has equivalent number of row weight 2 and 3 rows. In Fig. 9, it can be seen that the non-binary LDPC convolutional code with  $J = 3$  outperforms the block codes like the binary case [8]. On the other hand, the non-binary LDPC convolutional code with  $J = 2$  have slightly worse performance than the corresponding

TABLE I  
BP THRESHOLD VALUES OF (2,4) AND (3,6) REGULAR LDPC CONVOLUTIONAL CODES (CC) AND BLOCK CODES (BC) OVER  $GL(GF(2), p)$ . COUPLING FACTORS  $L$  [14] OF CC IS 64.

$p$	(2,4) CC	(2,4) BC	(3,6) CC	(3,6) BC
1	0.333333	0.333333	0.4881	0.4294
2	0.409912	0.409604	0.490723	0.423472
3	0.453491	0.450595	0.49353	0.412203
4	0.474976	0.468011	0.494629	0.398902
5	0.48584	0.474147	0.496094	0.385472
6	0.490234	0.47464		

block codes. Lentmaier *et al.* describes that BP thresholds of regular LDPC convolutional codes improve by increasing  $J$  in [13]. Kudekar *et al.* investigated such decoding performance improvement by using GEXIT and showed that the LDPC convolutional coding increases the BP threshold up to the MAP threshold of the underlying block code [6]. Kudekar *et al.* called this phenomenon *threshold saturation* [14]. From the above discussion, we consider that the BP threshold of the  $J = 2$  non-binary LDPC block code is already very close to its MAP threshold, so that the corresponding convolutional code cannot outperform in the simulation. In order to verify the consideration, we will compute the BP threshold.

Since density evolution over the AWGN channel for non-binary LDPC codes with large field size becomes computationally intensive and tractable only for the BEC, we will calculate the BP thresholds over BEC by using density evolution for the non-binary LDPC code ensembles with parity-check matrices defined over the general linear group  $GL(GF(2), p)$  [15], instead of Galois field. This is a fair approximation, since in [15], it is reported that the threshold for the code ensemble with parity-check matrices defined over  $GF(2^p)$  and  $GL(GF(2), p)$  have almost the same thresholds within the order of  $10^{-4}$ . We follow an ensemble representation of non-binary LDPC convolutional codes in [14] for density evolution. The BP thresholds of non-binary LDPC convolutional and block codes over binary erasure channel (BEC) are shown in Table I. It can be observed that both BP thresholds of (2,4) regular LDPC convolutional and block codes are almost same at the identical  $p$ . On the other hand, a BP threshold of (3,6) regular LDPC convolutional codes is increasing with increasing  $p$ , however that of block codes is decreasing. This result implies that it is easier to see threshold saturation for the (3,6) regular LDPC convolutional codes at a moderate length than the (2,4) regular LDPC convolutional codes. Since the BP threshold of (2,4) regular LDPC convolutional codes is slightly higher than that of the block code at the large  $p$ , we believe the threshold saturation could be observed with sufficiently large lengths.

#### IV. RATE-COMPATIBILITY OF NON-BINARY LDPC CONVOLUTIONAL CODES

In this section, we discuss rate-compatibility of non-binary LDPC convolutional codes. Rate-compatible non-binary LDPC convolutional codes are defined over  $GF(2^8)$  in this section for convenience. For non-binary LDPC block

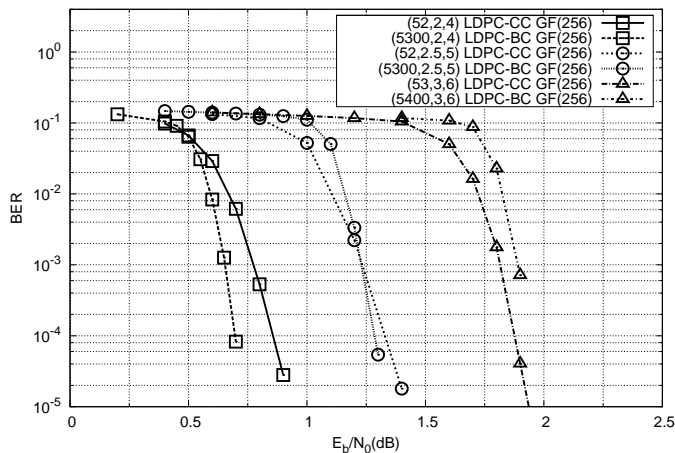


Fig. 9. Simulation results of  $(m_s, J, K)$  LDPC convolutional codes (CCs) of different degrees of symbol nodes and  $(N, J, K)$  block codes (BCs) with comparable memory requirements. All of these codes are of rate 1/2 and defined over  $\text{GF}(2^8)$ . The performance of the CC becomes better than that of the BC with increasing  $d_v$ .

codes, puncturing and multiplicative repetition give good rate-compatibility [5]. We show that those techniques are also applicable in non-binary LDPC convolutional codes.

An encoder structure of a rate-compatible non-binary LDPC convolutional code is shown in Fig. 10. This encoder is composed of an encoder of a mother code  $\mathcal{C}_1$ , a puncturing unit and multiplicative repeaters. Coefficients  $\alpha_t^{(1)}, \alpha_t^{(2)}, t = 0, \dots, N + Z - 1$  are chosen randomly from  $\text{GF}(2^8) \setminus \{0, 1\}$ . The mother code  $\mathcal{C}_1$  is the non-binary LDPC convolutional code discussed in the previous section, and the encoding process is accomplished with shift registers. The information symbols  $u_t \in \text{GF}(2^8)$  enter the encoder. The corresponding encoded symbols of the  $\mathcal{C}_1$  encoder are given by  $(v_t^{(1)}, v_t^{(2)})$ . The encoder is systematic, i.e.,  $v_t^{(1)} = u_t$ .

By puncturing the parity symbols  $v_t^{(2)}$  for  $t = 0, \dots, N + Z - 1$ , the coding rate increases. Some puncturing patterns used in the simulation are shown in Table II. On the other hand, by multiplicatively repeating the encoded symbols  $(v_t^{(1)}, v_t^{(2)})$  with multiplicative repetition coefficient  $(\alpha_t^{(1)} v_t^{(2)}, \alpha_t^{(1)} v_t^{(2)})$ , the coding rate decreases down to 1/4. The more we increase multiplicatively repeated symbols, the more overall rate decreases. We can also design various rates with combining puncturing and multiplicative repetition.

Figures 11 and 12 describe the Tanner graph of a (5,2,4)-regular LDPC convolutional code used for decoding procedure with punctured symbols and multiplicatively repeated symbols, respectively. The coding rates are 3/4 and 1/4, respectively.

For the puncturing case in Fig. 11, channel likelihoods of the puncturing nodes (blue nodes) are initialized with uniform probability, then the iterative decoding process proceeds on the mother Tanner graph. For the multiplicative repetition case in Fig. 12, multiplicatively repeated nodes (green nodes) send each message just once before the decoding process starts, then iterative decoding proceeds on the mother Tanner graph.

In both cases, the decoder uses only the mother Tanner graph. Hence, we do not need to change the decoder architecture for all rates.

Figure 13 shows the performance of rate-compatible non-binary LDPC convolutional codes. The mother code is a (52, 2, 4) LDPC convolutional code over  $\text{GF}(2^8)$ , which is evaluated in Section III-B.

The mother code of the rate 1/2, multiplicatively repeated code of the rate 1/4, puncturing codes for rates = 3/4, 5/6, and 7/8 have bit error rate  $10^{-4}$  around at  $E_b/N_0 = 0.9$  dB, 0.05 dB, 2.2 dB, 3 dB, and 3.5 dB, while the Shannon limits of the binary-input AWGN for rates 1/2, 1/4, 3/4, 5/6, and 7/8 are 0.187 dB, -0.794 dB, 1.626 dB, 2.362 dB, and 2.845 dB, respectively. As shown in these curves, the proposed rate-compatible non-binary convolutional code, although simple, can be constructed from low rates to high rates without large loss from the Shannon limits.

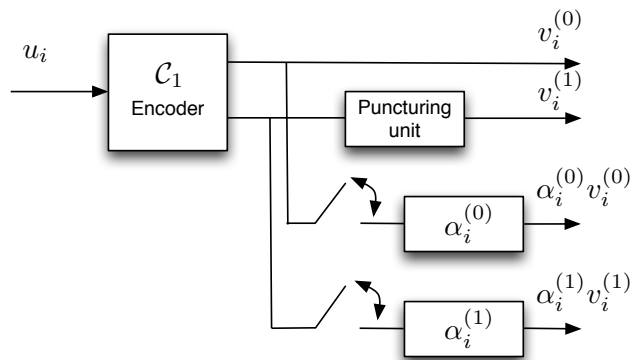


Fig. 10. An encoder structure of the proposed rate-compatible non-binary LDPC convolutional code

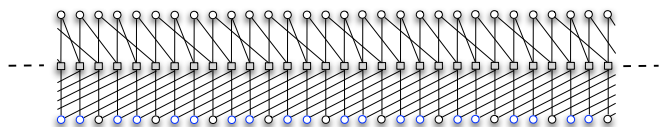


Fig. 11. Tanner graph of a (5,2,4)-regular LDPC convolutional code of rate 3/4 with puncture bits. Blue nodes are punctured nodes.

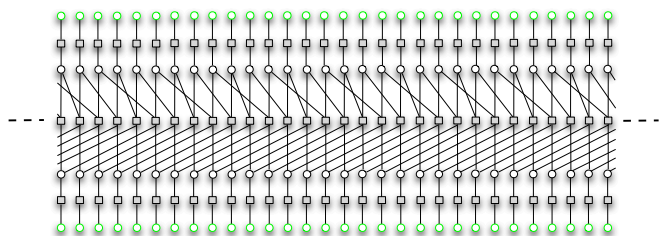


Fig. 12. Tanner graph of a (5,2,4)-regular LDPC convolutional code of rate 1/4 with multiplicative repetition. Green nodes are multiplicative repetition nodes.

TABLE II  
PUNCTURING PATTERNS OF R= 3/4, 5/6, AND 7/8. THE \* REPRESENTS THE PUNCTURED SYMBOL AND R=1/2 IS A REFERENCE.

R	sequence
1/2	$v_t^{(1)}, v_t^{(2)}, v_{t+1}^{(1)}, v_{t+1}^{(2)}, v_{t+2}^{(1)}, v_{t+2}^{(2)}, \dots$
3/4	$v_t^{(1)}, *, v_{t+1}^{(1)}, *, v_{t+2}^{(1)}, v_{t+2}^{(2)}, \dots$
5/6	$v_t^{(1)}, *, v_{t+1}^{(1)}, *, v_{t+2}^{(1)}, *, v_{t+3}^{(1)}, *, v_{t+4}^{(1)}, v_{t+4}^{(2)}, \dots$
7/8	$v_t^{(1)}, *, v_{t+1}^{(1)}, *, v_{t+2}^{(1)}, *, v_{t+3}^{(1)}, *, v_{t+4}^{(1)}, *, v_{t+5}^{(1)}, *, v_{t+6}^{(1)}, v_{t+6}^{(2)}, \dots$

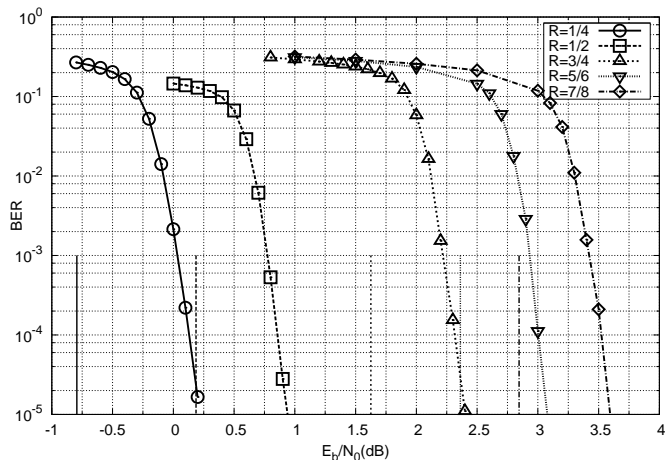


Fig. 13. Simulation results for rate-compatibility of non-binary LDPC convolutional codes over  $GF(2^8)$  of rates 1/4, 1/2, 3/4, 5/6, and 7/8 (marked curves). Corresponding Shannon limits to the rates are also described (vertical lines).

## V. CONCLUSIONS

In this paper, we introduced terminated non-binary low-density parity-check (LDPC) convolutional codes and gave a construction method of a syndrome former matrix. Moreover we discussed the rate-compatibility of the non-binary LDPC convolutional codes. Simulation results showed that non-binary LDPC convolutional codes of rate 1/2 outperform binary LDPC convolutional codes with smaller decoding latency. Also the derived non-binary LDPC convolutional codes have good performance for rates from 1/4 to 7/8 without large loss from the Shannon limits.

However the non-binary LDPC block code outperforms the corresponding non-binary LDPC convolutional code for the same memory requirements. The density evolution results implied that it is because the MAP threshold and the BP threshold are very close for  $J = 2$  regular non-binary LDPC codes. Since the BP threshold of (2,4) regular LDPC convolutional codes seems to be slightly higher than that of the block code at the large field size, we believe the threshold saturation could be observed with sufficiently large lengths.

## REFERENCES

- [1] A. J. Felström and K. S. Zigangirov, "Time-varying periodic convolutional codes with low-density parity-check matrix," *IEEE Trans. on Inform. Theory*, vol. 45, no. 6, pp. 2181–2191, 1999.
- [2] R. G. Gallager, "Low-density parity-check codes," *IRE Trans. Inform. Theory*, vol. IT-8, pp. 21–28, 1962.

- [3] T. J. Richardson, M. Shokrollahi, and R. Urbanke, "Design of capacity-approaching irregular low-density parity-check codes," *IEEE Trans. on Inform. Theory*, vol. 47, pp. 619–637, 2001.
- [4] M. C. Davey and D. J. MacKay, "Low density parity check codes over  $GF(q)$ ," *IEEE Communications Letters*, vol. 2, pp. 70–71, 1996.
- [5] K. Kasai, D. Declercq, C. Poulliat, and K. Sakaniwa, "Multiplicatively repeated non-binary LDPC codes," *accepted to IEEE Transactions on Information Theory*, 2011.
- [6] S. Kudekar, C. Méasson, T. J. Richardson, and R. Urbanke, "Threshold saturation on BMS channels via spatial coupling," in *The 6th International Symposium on Turbo Codes and Related Topics*, September 2010, pp. 319–323, brest France.
- [7] M. Papaleo, A. R. Iyengar, P. H. Siegel, J. K. Wolf, and G. E. Corazza, "Windowed erasure decoding of LDPC convolutional codes," in *Information Theory Workshop (ITW)*, January 2010, pp. 78–82, cairo Egypt.
- [8] D. Costello, A. Pusane, S. Bates, and D. Divsalar, "A comparison between LDPC block and convolutional codes," in *Information Theory and Applications Workshop, 2006*, February 2006.
- [9] A. E. Pusane, K. S. Zigangirov, and D. J. C. Jr., "Construction of irregular LDPC convolutional codes with fast encoding," in *IEEE International Conference on Communications (ICC06)*, June 2006, pp. 1160–1165.
- [10] C. Poulliat, M. Fossorier, and D. Declercq, "Design of regular  $(2, d_c)$ -LDPC codes over  $GF(q)$  using their binary images," *IEEE Transactions on Communications*, vol. 56, no. 10, pp. 1626–1635, October 2008.
- [11] V. Savin, "Non binary LDPC codes over the binary erasure channel: Density evolution analysis," in *First International Symposium on Applied Sciences on Biomedical and Communication Technologies (ISABEL)*, October 2008, pp. 1–5.
- [12] M. Lentmaier, D. Mitchell, G. Fettweis, and D. Costello, "Asymptotically good LDPC convolutional codes with AWGN channel thresholds close to the Shannon limit," in *The 6th International Symposium on Turbo Codes and Iterative Information Processing*, 2010, pp. 334–338, brest France.
- [13] M. Lentmaier, A. Sridharan, D. J. C. Jr., and K. S. Zigangirov, "Iterative decoding threshold analysis for LDPC convolutional codes," *IEEE Transactions on Information Theory*, vol. 56, no. 10, pp. 5274–5289, 2010.
- [14] S. Kudekar, T. Richardson, and R. Urbanke, "Threshold saturation via spatial coupling: Why convolutional LDPC ensembles perform so well over the BEC," *IEEE Transactions on Information Theory*, vol. 57, no. 2, pp. 803–834, February 2011.
- [15] V. Rathi and R. Urbanke, "Density Evolution, Threshold and the Stability Condition for non-binary LDPC Codes," *IEE Proceedings - Communications*, vol. 152, no. 6, pp. 1069–1074, 2005.